

GA-A23165

**EVOLUTION OF 2D VISIBLE AND VUV
DIVERTOR EMISSION PROFILES DURING
DIII-D H-MODE DETACHMENT TRANSITIONS**

by

**M.E. FENSTERMACHER, N. JALUFKA, W.H. MEYER,
D.G. NILSON, J. GAFERT, J. HOGAN, C.J. LASNIER,
A.W. LEONARD, R.A. PITTS, G.D. PORTER, and the DIII-D TEAM**

JULY 1999

DISCLAIMER

This report was prepared as an account of work sponsored by an agency of the United States Government. Neither the United States Government nor any agency thereof, nor any of their employees, makes any warranty, express or implied, or assumes any legal liability or responsibility for the accuracy, completeness, or usefulness of any information, apparatus, product, or process disclosed, or represents that its use would not infringe privately owned rights. Reference herein to any specific commercial product, process, or service by trade name, trademark, manufacturer, or otherwise, does not necessarily constitute or imply its endorsement, recommendation, or favoring by the United States Government or any agency thereof. The views and opinions of authors expressed herein do not necessarily state or reflect those of the United States Government or any agency thereof.

EVOLUTION OF 2D VISIBLE AND VUV DIVERTOR EMISSION PROFILES DURING DIII-D H-MODE DETACHMENT TRANSITIONS

by

M.E. FENSTERMACHER,* N. JALUFKA,† W.H. MEYER,*
D.G. NILSON,* J. GAFERT,‡ J. HOGAN,△ C.J. LASNIER,*
A.W. LEONARD, R.A. PITTS,# G.D. PORTER,* and the DIII-D TEAM

This is a preprint of a paper presented at the Twenty-Sixth European Physical Society Conference on Controlled Fusion and Plasma Physics, June 14–18, 1999 in Maastricht, The Netherlands, and to be published in *The Proceedings*.

*Lawrence Livermore National Laboratory, Livermore, California.

†Hampton University, Hampton, Virginia.

‡Max-Planck Institut for Plasmaphysik, EURATOM Association, Garching, Germany.

△Oak Ridge National Laboratory, Oak Ridge, Tennessee.

#CRPP, Association EURATOM-Confederation Suisse, Lausanne, Switzerland.

Work supported by
the U.S. Department of Energy
under Contract Nos. W-7405-ENG, DE-AC03-99ER54463, DE-AC05-
96OR22464, and Grant No. DE-FG03-95ER54294

GA PROJECT 30033
JULY 1999

Evolution of 2D Visible and VUV Divertor Emission Profiles During DIII–D H–Mode Detachment Transitions

M.E. Fenstermacher,^a N. Jalufka,^b W.H. Meyer,^a D.G. Nilson,^a J. Gafert,^c J. Hogan,^d C.J. Lasnier,^a A.W. Leonard, R.A. Pitts,^e G.D. Porter,^a and the DIII–D Team

General Atomics, San Diego California, USA

^a*Lawrence Livermore National Laboratory, P.O. Box 808, Livermore, California 94550*

^b*Hampton University, Hampton Virginia, USA*

^c*Max-Planck Institut fur Plasmaphysik, EURATOM Association, D-85748, Garching, Germany*

^d*Oak Ridge National Laboratory, Oak Ridge, Tennessee, USA*

^e*Centre de Recherches en Physique des Plasmas, Association EURATOM-Confederation Suisse, Ecole Polytechnique Federale de Lausanne, CH-1015, Lausanne, Switzerland*

The peak heat flux to divertor target surfaces (P_{div}) must be reduced, compared with present experimental levels, before a tokamak operating in the high confinement regime (H–mode) can be extrapolated to a reactor. Partially Detached Divertor (PDD) operation [1], in which deuterium gas is injected into an H–mode plasma, reduces P_{div} by factors of 3–5 in DIII–D. A key element in the physics model of PDD operation is that carbon radiation near the X–point dissipates the energy flowing in the scrape-off-layer (SOL) before it enters the divertor [2]. This allows the divertor temperature to be low, density to be high and thereby reduces the heat flux and ion particle flux to the targets both by reduced recycling and increased recombination. Previous line integrated SPRED measurements [3] and computer simulations indicated that the 155 nm $\Delta n = 0$ transition of C^{3+} was the main power radiator from carbon during PDD operation.

This paper presents the first 2D profiles of 155 nm CIV emission in any tokamak divertor. The images were obtained on DIII–D with a new tangentially viewing VUV camera [4] and established image reconstruction techniques [5]. The discharges were lower single null configurations with, $I_p = 1.75$ MA, $B_T = 2.1$ T, $q_{95} = 3.2$, $P_{\text{inj}} = 9$ MW, $\kappa = 1.9$ and the ∇B drift toward the lower divertor. After establishing an ELMing H–mode with neutral beam injection, deuterium gas was injected at 17 Pa m^3/s (130 T ℓ/s) to increase the divertor density and produce a transition to PDD operation. A typical discharge scenario is given in Ref. [2].

Profiles of the radiation from CIV (VUV camera), CIII (465 nm) and D_α (visible cameras [5]) and reconstructions of the total radiated power (P_{rad}) from a 48-channel bolometer array are shown in Fig. 1. The spatial profiles of the CIV and CIII emission are similar, both before deuterium injection [Figs. 1(a) and (b)], and during the late phases of PDD operation near the density limit [Figs. 1(e) and (f)]. Peak intensity is in the inner SOL at the height of the X–point before gas injection and inside the closed flux surfaces above the X–point when the plasma reaches the density limit.

Previous VUV spectrometer measurements [3,2] integrated vertically through the divertor indicated that near the X–point during PDD operation CIV contributes 50% and deuterium contributes 20% of P_{rad} . Near the outer strikepoint (OSP) deuterium contributes 60% and CIV 25% of P_{rad} . Comparing the uncalibrated 2D emission profile in Fig. 1(e) weighted by these ratios with the P_{rad} profile [Fig. 1(g)] shows that the peak in P_{rad} near the X–point is consistent with the CIV profile. The D_α profile in Fig. 1(g) shows deuterium emission contributes to the P_{rad} peaks at the two strikepoints but the D_α profile would also imply more P_{rad}

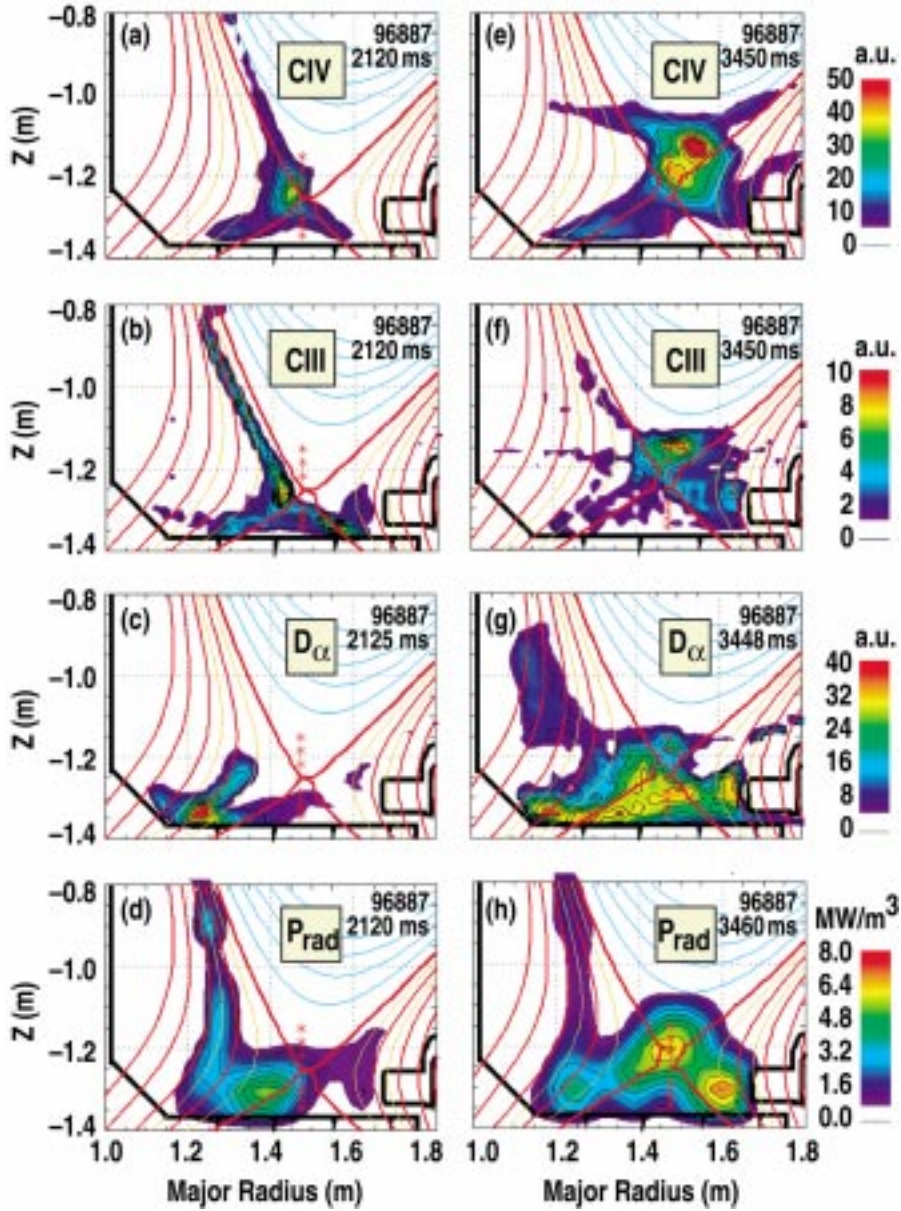


Fig. 1. Profiles before (a–d) and during (e–h) PDD operation of emission from CIV (a,e), CIII (b,f), D_{α} (c,g) and total radiated power from bolometer measurements (d,h).

in the private flux (PF) region below the X–point than seen and less peaked emission at the OSP. Singly ionized carbon radiation may contribute at the OSP.

Two-dimensional profiles of T_e and n_e from divertor Thomson scattering (DTS) measurements [6] for the PDD phase of a similar discharge are shown in Fig. 2. The relative position of the CIV and CIII peak intensities in Fig. 1 are consistent with the T_e gradients from the DTS profile near the X–point in that the CIV emission appears slightly farther up along the separatrix toward the midplane and therefore at slightly higher temperature. The temperatures at the radiation locations for CIV and CIII which are consistent with line integrated SPRED measurements [3,2] are (~ 8 – 12 eV) for CIV and (~ 5 – 8 eV) for CIII. This unexpected result that the profiles of VUV CIV ($\Delta n = 0$ transition) and visible CIII ($\Delta n \neq 0$, temperature sensitive transition) are very similar is due to the large spatial gradients of T_e in this temperature range during PDD. Time sequence animations of multiple frames from several discharges showing the transition from pre-gas H–mode to PDD operation and, with

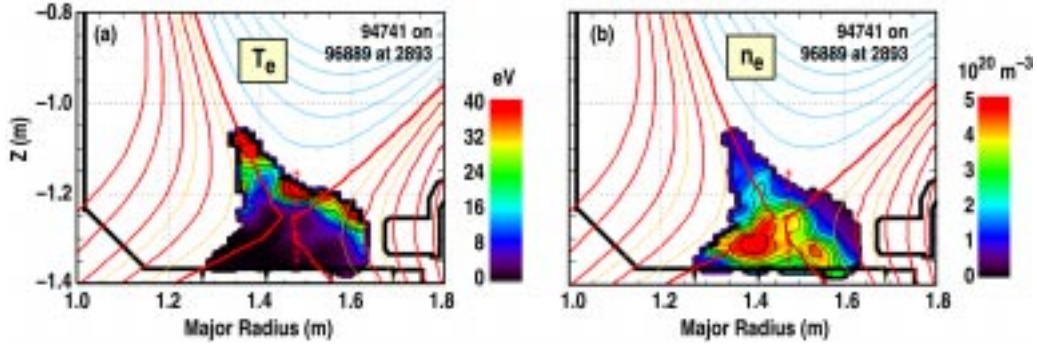


Fig. 2. Profiles of (a) electron temperature and (b) electron density from DTS measurements during PDD operation.

continued heavy gas injection, to the H–L density limit at the H–L back transition confirm that the spatial distribution of CIV emission is a good proxy for the main carbon radiator, CIV in the DIII–D divertor.

Profiles of CIV emission during the transition from pre-gas H–mode to the high density phases of PDD operation are shown in Fig. 3. As seen previously in CIII images [7] the first effect of gas injection is the appearance of emission near the X–point and in the upper regions of the outer leg [Fig. 3(a)]. Fully established PDD operation shows localized emission in the outer SOL at the X–point [Fig. 3(b)]. Continued high level gas puffing pushes the partially detached divertor to high enough density and low enough temperature that the carbon emission begins to move inside the closed flux surfaces [Fig. 3(c)]. Substantial core energy confinement degradation occurs at this stage [8] and at slightly higher density the profile of Fig. 1 is obtained at the H–L density limit.

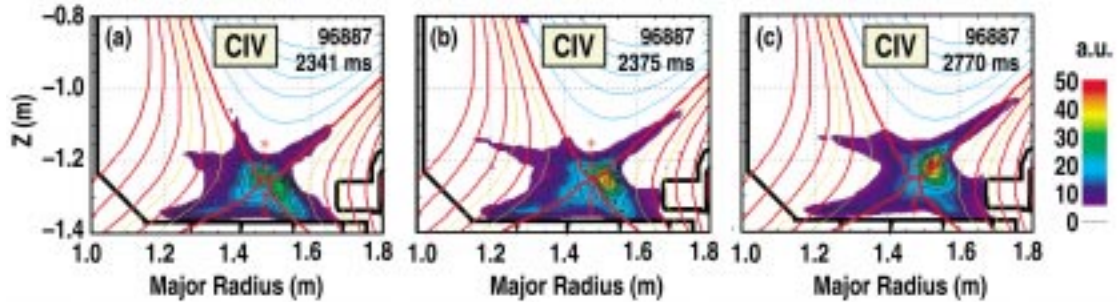


Fig. 3. Evolution of CIV emission profiles from (a) onset of PDD transition at 140 ms after gas injection, (b) established PDD operation and (c) onset of CIV radiation inside the separatrix and core confinement degradation after continued heavy gas injection.

The deuterium emission profile also evolves throughout various phases of PDD operation. The profiles of Fig. 1 show the typical transition from emission near the inner strikepoint in pre-gas H–mode to distributed emission throughout the divertor including in the PF region and the lower regions of the outer leg during PDD operation. Analysis of multiple simultaneous images of different Balmer series lines allows the D_α emission due to recombination to be separated from that due to ionization [7]. The emission in the PF region is typically associated with recombination, consistent with the very low T_e (~ 0.5 – 1.0 eV) and high n_e (~ 2 – 4×10^{20} m^{-3}) measured there (Fig. 2). In some cases, however, the emission in the PF region is not seen. Figures 4(a) and 4(b) show a comparison of D_α emission attributable to recombination during PDD operation in a discharge for which the injected power was 7 MW (170 Hz ELMs) and 2 MW (40 Hz ELMs) respectively. Core plasma pedestal profiles show that the plasma remains in H–mode even at the lower power. Animations of this emission show a smooth transition in which the D_2 emission in the PF region disappears after the power and ELM

frequency are reduced. The ELM model in the B2-Eirene SOL and divertor code [9] is capable of simulating this transition. Work continues to determine if transport of particles and energy into the PF region due to the ELMs can explain the observed emission there.

In conclusion, comparison of the CIV VUV profiles with CIII visible profiles supports previous conclusions [2] that the CIII emission gives a good indication of the spatial profile of carbon radiation because it is located very near the region of high radiated power CIV emission especially during PDD operation. The profile of the VUV CIV emission evolves during the transition to PDD operation, starting from 1) localized emission in the inner SOL at the X-point height moving to 2) the outer SOL above the X-point and then 3) into the closed flux surfaces above the X-point at the H-L density limit. Animations of the 2D profiles of D_α emission show 1) separated regions of recombination and ionization [7], and 2) substantial emission in the PF region during the transition to PDD for H-mode discharges with high ELM frequency; reduced PF emission at lower power and ELM frequency. These detailed 2D divertor emission profiles will provide benchmarks for SOL/divertor codes which will increase our confidence in their use to predict divertor behavior in future high power tokamaks.

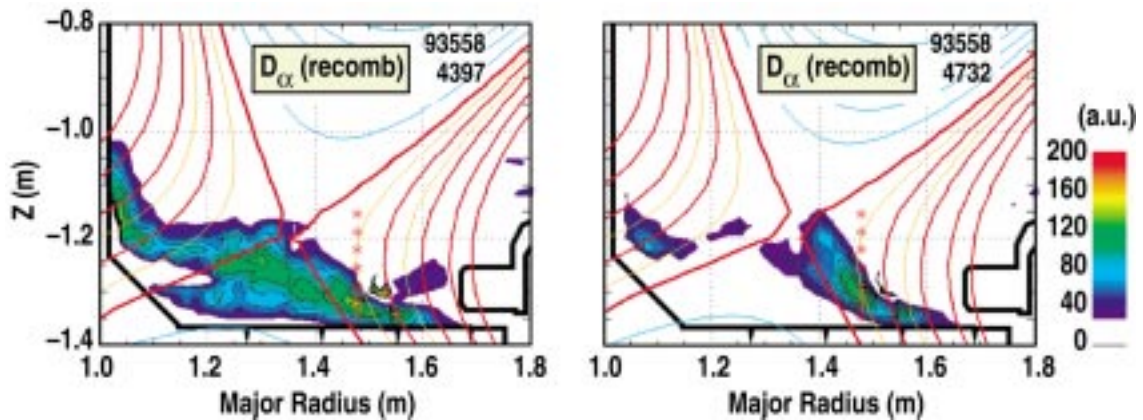


Fig.4. Profiles of D_α emission due to recombination during PDD operation with (a) $P_{inj} = 7$ MW and (b) $P_{inj} = 2$ MW showing reduced emission in the private flux region at low power.

This work was supported by U.S. Department of Energy under Contract Nos. W-7405-ENG-48, DE-AC03-99ER54463, DE-AC05-96OR22464 and Grant DE-FG03-95ER54294.

- [1] T.W. Petrie, *et al.*, in Proc. 18th Euro. Conf. on Contr. Fusion and Plasma Phys., Berlin, Germany, Vol. 15C, Part II (European Physical Society, Petit-Lancy: 1991) p. 237.
- [2] M.E. Fenstermacher, *et al.*, Phys. Plasmas **4** (1997) 1761, M.E. Fenstermacher, *et al.*, Plasma Phys. and Contr. Fusion **41** (1999) 345.
- [3] R.D. Wood, *et al.*, in Proc. 23rd Euro. Conf. On Plasma Phys. and Contr. Fusion, Kiev, Vol. 20C, Part II (European Physical Society, 1996) p. 763.
- [4] D.G. Nilson, *et al.*, Rev. Sci. Instrum. **70** (1999) 738.
- [5] M.E. Fenstermacher, Rev. Sci. Instrum. **68** (1997) 974.
- [6] D.G. Nilson, T.N. Carlstrom, *et al.*, Fusion Eng. Design (Proc Toki Conf 1995).
- [7] M.E. Fenstermacher, *et al.* J. Nucl. Mater. **266-269** (1999) 348.
- [8] T.W. Petrie, *et al.* J. Nucl. Mater. **241-243** (1997) 639.
- [9] D. Reiter, *et al.*, J Nucl. Mater., **220-222** (1995) 987; J. Hogan, *et al.*, Proc. of 25th Euro. Conf. on Contr. Fusion and Plasma Phys., Prague, Vol., 22C (European Physical Society, Petit-Lancy, Switzerland, 1998) B020PR